

Early Cenozoic decoupling of the global carbon and sulfur cycles

A. C. Kurtz,¹ L. R. Kump,² M. A. Arthur,² J. C. Zachos,³ and A. Paytan⁴

Received 3 April 2003; revised 25 July 2003; accepted 22 September 2003; published 4 December 2003.

[1] Changes in carbon and sulfur cycling over geologic time may have caused considerable modification of atmospheric and oceanic composition and climate. Here we calculate pyrite sulfur (S_{py}) and organic carbon (C_{org}) burial rates from recently improved Cenozoic stable isotope records, and from these rates we infer global changes in C_{org} burial environments. Given predominantly normal shelf-delta organic carbon burial, the global S_{py} burial flux should be coupled to C_{org} burial. However, we find that the major early Cenozoic peak in C_{org} burial coincides with a minimum in S_{py} burial. Although the calculated magnitude of variations in global pyrite burial flux is sensitive to our assumptions about the concentration of sulfate in paleoseawater, a non-steady-state isotope mass balance model indicates very low S_{py} burial rates during the Paleocene and a dramatic increase starting near the Paleocene-Eocene boundary, dropping off to a fairly constant Cenozoic rate beginning in the middle Eocene. High C_{org}/S_{py} burial ratios (C/S mole ratio $\approx 15-30$) coinciding with the Paleocene carbon isotope maximum most likely reflect enhanced accumulation of terrestrial organic carbon in Paleocene terrestrial swamps. We suggest that rapid burning of accumulated Paleocene terrestrial organic carbon could have significantly contributed to the short-lived negative carbon isotope excursion at the Paleocene-Eocene boundary in addition to or possibly even as an alternative to release of gas hydrates from the continental slopes. An early Eocene minimum in calculated C_{org}/S_{py} burial ratios (C/S mole ratio $\approx 2-4$) suggests that the predominant locus of organic carbon burial shifted to euxinic environments in a warm early Eocene ocean. *INDEX TERMS*: 4805 Oceanography: Biological and Chemical: Biogeochemical cycles (1615); 4806 Oceanography: Biological and Chemical: Carbon cycling; 4842 Oceanography: Biological and Chemical: Modeling; 1040 Geochemistry: Isotopic composition/chemistry; *KEYWORDS*: carbon burial, sulfur, Paleogene

Citation: Kurtz, A. C., L. R. Kump, M. A. Arthur, J. C. Zachos, and A. Paytan, Early Cenozoic decoupling of the global carbon and sulfur cycles, *Paleoceanography*, 18(4), 1090, doi:10.1029/2003PA000908, 2003.

1. Introduction

[2] The most prominent feature of the Cenozoic carbon isotope record, the “Paleocene carbon isotope maximum,” began ~ 2 m.y. after the Cretaceous-Tertiary boundary, peaked in the middle Paleocene (C25N–C26N), and waned through the late Paleocene and into the early Eocene [Shackleton and Hall, 1984; Miller et al., 1987]. This excursion has been interpreted as evidence for an increased rate of organic carbon (C_{org}) burial maintained for roughly 10 million years [e.g., Shackleton, 1987]. Superimposed on the waning stages of the carbon isotope maximum is a prominent short-term negative carbon isotope excursion at ~ 55 Ma associated with the Paleocene-Eocene Thermal Maximum (PETM). One explanation for this feature is the rapid release of methane from gas hydrates in continental slope sediments [Dickens et al., 1995], resulting in a major

short-term perturbation to the Earth’s carbon cycle and climate.

[3] Because the marine and terrestrial carbon cycles are coupled through atmospheric CO_2 , the Paleocene carbon isotope maximum might reflect an increase in C_{org} burial in either marine or terrestrial environments. A number of studies [Shackleton et al., 1984; Oberhansli and Hsu, 1986; Corfield and Cartlidge, 1992; Corfield, 1994, 1998; Bralower et al., 1995] have shown that the Paleocene carbon isotope maximum is observed in both planktonic and benthic marine carbon isotope records. Furthermore, the magnitude of the oceanic vertical carbon isotope gradient may have increased as $\delta^{13}C$ values become more positive. Corfield and Cartlidge [1992] interpret this as an indication of increased marine productivity during the Paleocene. Thompson and Schmitz [1997] argued, on the basis of marine sedimentary barium concentrations, for a large late Paleocene increase in marine organic carbon burial (6-fold) in oligotrophic regions of the oceans, and a much smaller increase (1.6-fold) in highly productive regions. An alternative explanation is that the Paleocene carbon isotope maximum was driven by an increase in terrestrial productivity and organic carbon burial [Oberhansli and Perch-Nielsen, 1990]. In this paper we argue that the Cenozoic sulfur isotope record [Paytan et al., 1998] can help us resolve the locus of organic carbon burial and the Paleocene-Eocene evolution of the global carbon cycle.

¹Department of Earth Sciences, Boston University, Boston, Massachusetts, USA.

²Department of Geosciences and NASA Astrobiology Institute, Pennsylvania State University, University Park, Pennsylvania, USA.

³Earth Sciences Department, University of California, Santa Cruz, California, USA.

⁴Department of Geological and Environmental Sciences, Stanford University, Stanford, California, USA.

Cenozoic carbon and sulfur cycles at steady state

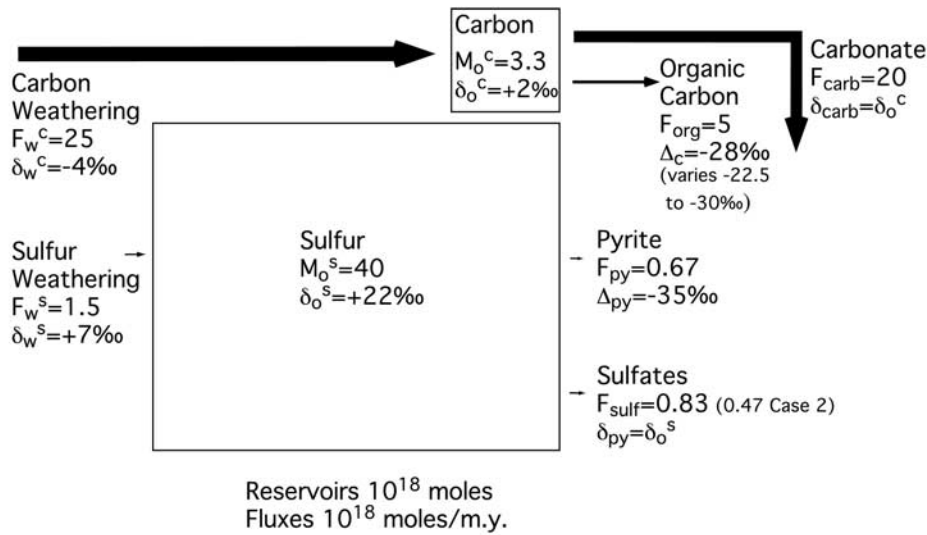


Figure 1. Illustration of box models for carbon and sulfur cycles used to calculate burial histories of C_{org} and S_{py} . Area of boxes was scaled to reservoir size, arrows were scaled to magnitude of fluxes. The carbon cycle is comprised of a small reservoir with large input and output fluxes, while the sulfur cycle is a large reservoir with very small fluxes. The difference is significant in terms of understanding their dynamics.

[4] Most previous studies of the relationship between the carbon and sulfur cycles [e.g., *Veizer et al.*, 1980; *Berner and Raiswell*, 1983; *Kump and Garrels*, 1986; *Carpenter and Lohmann*, 1997; *Petsch and Berner*, 1998] have been concerned with long time scales (>10 m.y.), over which steady state assumptions are justified, and where carbon-sulfur-oxygen feedbacks are able to adjust to perturbations. *Paytan and Arrigo* [2000] were the first to take advantage of the availability of relatively high-resolution (~1 m.y.) Cenozoic carbon and sulfur isotope records to examine the evidence for coupling between the C, S, and O cycles on much shorter timescales. Here we focus on the relationship between early Cenozoic C_{org} and S_{py} burial fluxes and organic carbon burial environments as calculated from the respective seawater isotope curves for these elements.

2. Cenozoic Organic Carbon and Pyrite Burial

2.1. Modeling the Carbon and Sulfur Cycles

[5] The principal control on $\delta^{13}C$ of marine dissolved inorganic carbon (DIC) is the fraction of carbon delivered to the exogenic cycle that is buried as organic carbon (C_{org}) versus carbonate. Similarly, the major control over the $\delta^{34}S$ of marine dissolved sulfate is the fractional burial flux of marine sulfur as biogenic pyrite (S_{py}) versus evaporite sulfate (gypsum/anhydrite) or pore water sulfate. We use simple models of the global carbon and sulfur cycles, each consisting of a single reservoir, one input, and two outputs (Figure 1) to interpret trends in the isotope records. In contrast to many previous treatments, the two cycles are not coupled through either a constant C/S sedimentary burial ratio [*Kump and Garrels*, 1986] or a productivity-

anoxia function [*Petsch and Berner*, 1998]. Instead, we use the simple box models to independently invert Cenozoic C and S isotopic records for possible histories of the Cenozoic C and S cycles, and in particular C_{org} and S_{py} burial rates. The calculated histories are subject to the assumptions of the simple box models and are not unique. However, driving the models with their respective isotope records allows us to examine the relationship between the two cycles.

[6] The single box for each element represents the mass and isotopic composition of carbon or sulfur in the exogenic cycle (global ocean, atmosphere, and terrestrial reservoirs). Following *Kump and Arthur* [1999], we group both volcanic and terrestrial weathering fluxes into a single input term for each that we refer to as “weathering” (F_w^C and F_w^S). Sedimentary outputs from the reservoir occur either as the oxidized form (carbonate (F_{carb}) or sulfate (F_{gyp})), or as the reduced form (organic carbon (F_{org}) or pyrite (F_{py})). Changes in the amount of carbon or sulfur in the exogenic system (M_o^C , M_o^S) result from long-term imbalances in weathering inputs and sedimentary outputs [*Garrels and Lerman*, 1984; *Kump and Garrels*, 1986]. This relationship is expressed in the equation below written in terms of carbon (equation (1a)) and sulfur (equation (1b)):

$$\frac{dM_o^C}{dt} = F_w^C - (F_{carb} + F_{org}) \quad (1a)$$

$$\frac{dM_o^S}{dt} = F_w^S - (F_{gyp} + F_{py}) \quad (1b)$$

A change in the input/output balance or form of output (carbonate/sulfate versus organic carbon/pyrite) will change the isotopic composition of the ocean/atmosphere reservoir (δ_0^C or δ_0^S):

$$\frac{d}{dt}(M_0^C \delta_0^C) = F_W^C \delta_W^C - F_{carb} \delta_0^C - F_{org}(\delta_0^C + \Delta_C) \quad (2a)$$

$$\frac{d}{dt}(M_0^S \delta_0^S) = F_W^S \delta_W^S - F_{gyp} \delta_0^S - F_{py}(\delta_0^S + \Delta_S) \quad (2b)$$

Here δ_W is the isotopic composition of the weathering (riverine) input of C or S. Delta (Δ) describes the average (biological) isotopic fractionation resulting from formation of organic carbon or pyrite from dissolved carbonate or sulfate, and is equivalent to the isotopic difference between sedimentary organic carbon versus carbonate or pyrite versus sulfate of the same geologic age. Substituting equation (1) into equation (2), we derive the time-dependent equation for the isotopic composition of the exogenic carbonate (equation (3a)) or sulfate (equation (3b)) reservoir:

$$\frac{d\delta_0^C}{dt} = \frac{F_W^C(\delta_W^C - \delta_0^C) - F_{org}\Delta_C}{M_0^C} \quad (3a)$$

$$\frac{d\delta_0^S}{dt} = \frac{F_W^S(\delta_W^S - \delta_0^S) - F_{py}\Delta_S}{M_0^S} \quad (3b)$$

Equation (3) expresses the assumption that the ocean is well mixed but does not require that either the mass or isotopic composition of the ocean be at steady state. It states that an imbalance in isotopic fluxes will cause an adjustment in the isotopic composition of the ocean. Note that the rate of change is inversely proportional to the amount of C or S in the reservoir. The implication is that the isotopic compositions of large reservoirs (e.g., oceanic sulfate) respond more slowly to a change in fluxes than relatively small reservoirs (e.g., oceanic inorganic C).

[7] Equation (3) can be solved for a steady state condition where the weathering input is balanced by the two outputs for each system, so there is no instantaneous change in either the mass or the isotopic composition of the reservoir. However, a steady state assumption is not applicable to timescales of change similar to or shorter than an element's residence time [e.g., *Kump and Garrels, 1986; Richter and Turekian, 1993*]. This becomes important when considering short timescale (Cenozoic) variations in sulfur isotopes, an element with a relatively long (>10 m.y.) residence time. The steady state approximation [e.g., *Paytan et al., 1998*] results in gross underestimates of transient maxima and minima in pyrite burial indicated by rapid changes in the sulfur isotope record during the early Paleogene. Rearranging equation (3), we solve for

F_{org} and F_{py} burial fluxes with no assumption of steady state:

$$F_{org} = \frac{F_W^C(\delta_W^C - \delta_0^C) - \frac{d\delta_0^C}{dt} M_0^C}{\Delta_C} \quad (4a)$$

$$F_{py} = \frac{F_W^S(\delta_W^S - \delta_0^S) - \frac{d\delta_0^S}{dt} M_0^S}{\Delta_S} \quad (4b)$$

Because fractionation of $\delta^{13}C$ and $\delta^{34}S$ are small during precipitation of sedimentary carbonate and sulfate, we can use sedimentary records of $\delta^{13}C_{carbonate}$ and $\delta^{34}S_{barite}$ as proxies for the changing isotopic composition of the exogenic carbon (δ_0^C) and sulfur (δ_0^S) reservoirs respectively. Isotope records from carbonate and sulfate sediments can be differentiated to provide the time rate of change of seawater carbon and sulfur isotopic compositions, i.e., the time-dependent term ($\frac{d\delta_0}{dt}$) in equation (4). M_0 appears explicitly in equation (4) and in general must be approximated, resulting in one additional source of uncertainty.

[8] We establish the boundary conditions for the model by assuming an average Cenozoic C_{org} burial flux of 5×10^{18} mol C/m.y. [*Kump and Arthur, 1997*] (Figure 1). Given a normal marine C_{org}/S_{py} burial ratio, (e.g., 7.5 molar ratio [*Berner and Raiswell, 1983; Raiswell and Berner, 1985, 1986*]), we calculate an average Cenozoic S_{py} burial flux of 0.67×10^{18} mol S/m.y. This estimate is close to the value suggested by *Holser et al. [1988]*, determined independently from the pyrite content of marine sediments. F_W and δ_W for carbon and sulfur are held constant at values consistent with this hypothetical Cenozoic steady state (Figure 1). Model values for Δ_C , photosynthetic carbon isotopic fractionation, are based on the *Hayes et al. [1999]* ϵ_{TOC} record. The curve is generally flat at -30‰ through the early Cenozoic and then increases approximately linearly to a modern value of -22.5‰ beginning around 30 Ma. A similar record is not available for sulfur, so we assume a constant value of -35‰ for Δ_S [*Kump and Garrels, 1986*]. We consider two end-member cases of seawater $[SO_4^{2-}]$ evolution. In the first we assume that the sulfate concentration of seawater (M_0^S) has been constant (28 mM) throughout the Cenozoic. F_W^S is held constant and F_{py} is calculated from isotopic mass balance. F_{gyp} is not explicitly considered because it does not affect the isotopic mass balance, and does not appear in equation (4). However, implicit in this calculation is that F_{gyp} varies inversely to F_{py} to maintain constant M_0^S .

[9] The concentration of sulfate in seawater (e.g., M_0^S) could change on million year timescales as a result of an imbalance between the weathering input and the pyrite and sulfate outputs. *Horita et al. [2002]* interpreted fluid inclusion data from early Eocene-Pliocene evaporites as evidence for a steady rise in seawater sulfate concentration from ~ 18 mM to present values of ~ 28 mM over the past 40 m.y. Similar data are not available for Paleocene evaporites, but *Lowenstein et al. [2001]* argue that the major

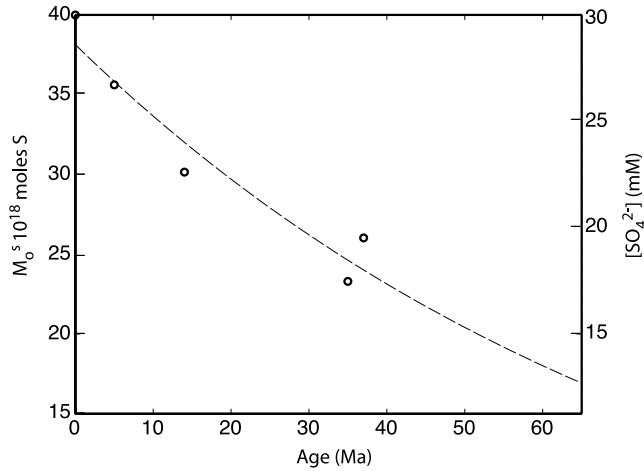


Figure 2. Open circles are estimates of seawater $[\text{SO}_4^{2-}]$ based on fluid inclusions in halite [Horita *et al.*, 2002]. Dashed line is an exponential fit to these data, used as Cenozoic evolution of seawater $[\text{SO}_4^{2-}]$ in “variable sulfate case” models.

element chemistry of seawater has been evolving from a low-sulfate, low Mg/Ca composition toward its present composition since the middle Cretaceous. Accordingly, in the second end-member model, we constrain the Cenozoic evolution of M_O^S with an exponential fit to the data of Horita *et al.* [2002] (Figure 2). As in the constant sulfate case, F_W^S is held constant, and F_{py} is calculated from isotopic mass balance (equation (4)). Again it is not necessary to explicitly consider F_{gyp} , but the rate of increase in M_O^S implies low (but nonzero) sulfate burial fluxes during the Cenozoic.

[10] The Cenozoic sulfur isotope record used in our model is based on Paytan *et al.* [1998], but with a revised age model (Figure 3). The Paytan *et al.* [1998] record was constructed from $\delta^{34}\text{S}$ measurements of sedimentary barite from eight DSDP and ODP cores plus Holocene core-top sediments. An updated age model (E. Thomas, personal communication, 2002) (Table 1) was constructed by consulting original DSDP/ODP biostratigraphic zone assignments for individual samples. Where necessary, zone assignments were updated for consistency with modern zonal concepts based on first and last appearance of key microfossil taxa. Numerical ages for datum levels are based on the work of Berggren *et al.* [1995].

[11] The revised age model differs significantly from the originally published version [Paytan *et al.*, 1998] only for the Eocene part of the record, but the difference is important. The updated age model indicates that the Eocene increase in $\delta^{34}\text{S}$ from ~ 17 to 22‰ occurs much more rapidly than originally indicated. This rapid rise is observed in both the Atlantic and Pacific oceans, recorded at three sites, east central North Atlantic site 366, and western North Pacific sites 305 and 577. Biostratigraphic ages at these three sites indicate a minimum in seawater $\delta^{34}\text{S}$ of 17.3‰ at 55.5 Ma. All three record the early Eocene initiation of the rise in $\delta^{34}\text{S}$ to 19.2‰ by 50 Ma. Site 366 sediments show that the steep rise in $\delta^{34}\text{S}$ from 18.1 to 22‰ occurs entirely

Table 1. Cenozoic Barite $\delta^{34}\text{S}$ Record With Revised Age Model¹

Location and Depth, m	Age, Ma	$\Delta^{34}\text{S}$, ‰ CDT
<i>Equatorial Pacific Surface^b</i>		
0–3	0.00	20.98
0–5	0.00	21.29
0–5	0.00	21.43
0–3	0.00	21.13
0–7	0.00	21.13
5–7	0.00	20.86
7–9	0.00	21.05
	0.40	20.90
<i>572A</i>		
4	0.24	21.21
33	2.20	22.02
68	4.70	22.24
104	5.50	22.05
141	6.10	22.34
<i>572D</i>		
163	6.80	22.32
210	7.80	22.25
234	8.30	22.10
258	8.70	22.17
314	11.60	22.72
314	11.60	22.69
334	11.80	22.70
<i>574A</i>		
10	2.13	22.02
10	2.13	22.00
37	5.81	21.96
55	7.64	21.76
55	7.64	21.96
75	9.40	21.90
102	12.40	22.10
151	13.91	22.10
<i>574C</i>		
237	17.87	21.90
294	20.52	21.56
313	21.45	22.01
348	23.53	21.90
354	24.32	21.86
367	25.60	21.70
378	26.38	21.90
378	26.38	21.79
378	26.38	21.41
397	28.05	21.26
418	28.05	21.52
418	28.05	21.35
444	30.87	21.39
475	32.83	21.60
498	33.27	21.99
501	33.80	22.43
501	33.80	22.50
520	34.62	22.50
520	34.62	22.53
<i>575B</i>		
7	1.38	21.90
27	8.38	21.80
33	9.50	21.90
33	9.47	21.96
34	9.66	21.98
38	10.38	22.24
43	10.74	22.18
47	11.68	22.09
55	12.48	22.00
58	12.64	21.73
76	13.71	21.97
82	14.11	22.10
93	14.75	22.00

Table 1. (continued)

Location and Depth, m	Age, Ma	$\Delta^{34}\text{S}$, ‰ CDT
102	15.37	21.96
102	15.37	21.79
119	16.39	22.09
575A		
149	18.87	21.80
	22.24	22.00
366		
414	34.10	21.40
415	34.40	22.64
435	35.20	22.16
454	35.80	22.14
472	38.70	22.61
511	39.50	22.47
522	40.70	22.20
530	41.00	22.10
551	42.50	22.40
605	49.10	22.00
644	49.70	21.60
644	49.70	21.55
662	50.20	20.30
682	50.70	19.16
688	50.80	18.09
720	53.80	17.72
720	53.80	17.76
729	55.40	17.27
748	55.80	18.02
305		
56	24.60	21.72
57	24.80	21.58
66	31.00	21.74
75	32.50	21.77
76	33.90	21.60
79	35.40	22.20
84	36.00	22.37
84	36.00	21.94
86	37.50	22.30
89	39.00	22.05
89	39.00	21.95
93	50.00	19.16
103	52.00	18.02
103	52.00	18.04
112	55.45	17.42
122	58.00	18.35
122	58.00	18.21
577		
41	3.58	21.58
50	4.85	21.78
60	5.90	21.63
63	34.50	21.81
69	49.53	19.31
69	49.53	19.31
78	52.82	18.40
78	52.82	17.51
81	55.50	17.19
88	56.54	17.72
90	57.23	17.55
92	57.91	18.00
92	57.91	17.95
92	57.91	18.03
96	59.62	18.15
101	62.20	18.60
102	62.40	19.09
103	62.49	19.05
103	62.49	19.18
106	63.86	18.81
106	63.86	19.19
107	64.21	18.96

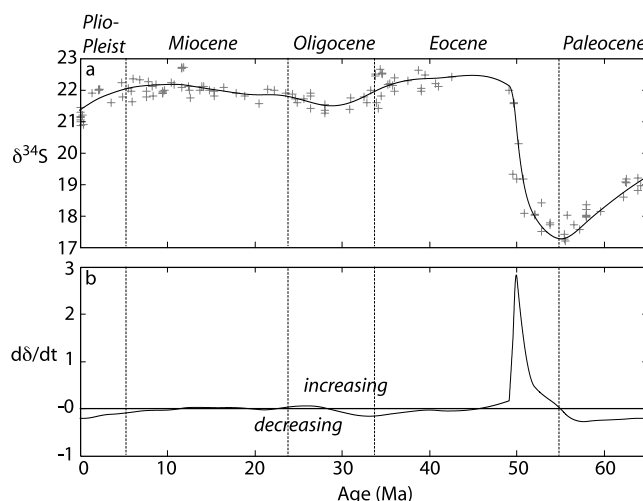


Figure 3. (a) Cenozoic sulfur isotope data modified from Paytan *et al.* [1998] plotted with crosses. Overlying curve was calculated by fitting a cubic smoothing spline to the data. (b) The first derivative of the smoothed sulfur curve. Positive values indicate periods during which the $\delta^{34}\text{S}$ of seawater was increasing, while negative values indicate periods during which the $\delta^{34}\text{S}$ of seawater was decreasing. Note that the rate of change is generally very small, consistent with a large, sluggish reservoir, except for the early Eocene when $\delta^{34}\text{S}$ rose by $>2.5\%$ /m.y.

within early Eocene nannoplankton zone NP12 (52.85–50.6 Ma [Berggren *et al.*, 1995]).

[12] The Cenozoic carbon isotope record (Figure 4) is based on the bulk carbonate $\delta^{13}\text{C}$ data from DSDP Leg 74 sediments (sites 525, 527, 528, 529) [Shackleton and Hall, 1984]. This record roughly mimics long and short-term trends in both benthic and planktonic $\delta^{13}\text{C}$ records and therefore provides a reasonable representation of how mean $\delta^{13}\text{C}$ evolves with time. In order to compare the carbon and sulfur isotope records, we revised the age model for Leg 74 record using the updated age assignments for magnetostratigraphic datum levels of Cande and Kent [1995].

[13] Solving equation (4a) requires both the isotopic records (δ_0) and their first derivatives ($\frac{d\delta_0}{dt}$). Differentiation of noisy data is problematic because insignificant wiggles in the primary data are amplified in the derivative curve. We addressed this problem by smoothing the carbon (Figure 4) and sulfur isotope records (Figure 3) with cubic smoothing splines, which are easily differentiated [deBoor, 1999]. Because the sulfur curve is sparsely sampled, we weighted some data points to force the smoothed curve through the rapidly changing early Eocene part of the record. We experimented with a range of spline stiffness parameters to find a value that preserved the first order features of the isotope records while minimizing perceived noise. Lacking

Notes to Table 1

^aData from Paytan *et al.* [1998] with revised biostratigraphic age model courtesy of E. Thomas (personal communication., 2002).

^bDepths for equatorial Pacific surface given in centimeters.

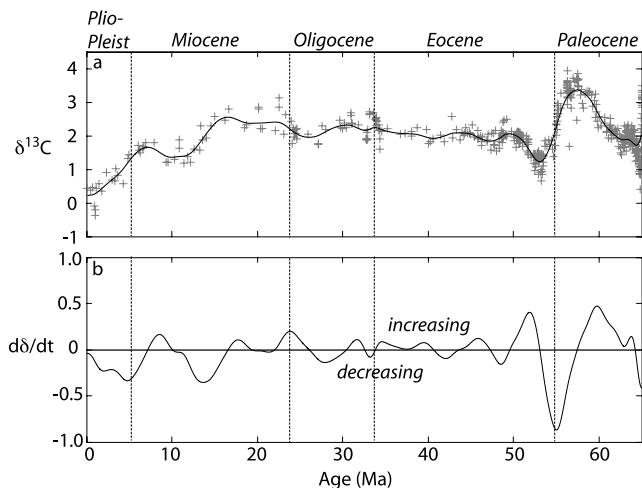


Figure 4. (a) Cenozoic carbon isotope record plotted with crosses. Record was constructed from the DSDP Leg 74 bulk sediment carbon isotope data [Shackleton and Hall, 1984] adjusted to the revised Cenozoic timescale of *Cande and Kent* [1995]. Overlying curve was calculated fitting a smoothing spline to the averaged data. (b) The first derivative of the smoothed curve in Figure 4a.

sufficient data for a statistically rigorous fit, the smoothed curves reflect a visual best fit to the data, and faithfully record the important features of the complete records.

2.2. Cenozoic Pyrite and Organic Carbon Burial Histories

[14] Organic carbon burial (calculated using equation (4a)) increases $\sim 25\%$ through the Paleocene to a peak corresponding to the “Paleocene carbon isotope maximum” (Figure 5a). Integrating F_{org} through this peak, and subtracting a constant organic carbon weathering flux of 5×10^{18} mol/m.y., we calculate net burial of 1.25×10^{18} moles of organic carbon during the Paleocene. Following this peak, organic carbon burial drops rapidly to an early Eocene minimum, and then rises steadily throughout the Cenozoic to a middle Miocene maximum.

[15] The pyrite burial rate (equation (4b)) exhibits transient maxima and minima indicated by rapid changes in the sulfur isotope record during the early Paleogene (Figure 5b). Because of the long residence time of sulfur (~ 25 m.y.), the Cenozoic sulfur isotope record represents a damped record of variations in global pyrite sulfur burial. Furthermore, the isotope record lags the pyrite-burial forcing by as much as 5 m.y. This is consistent with the arguments of *Richter and Turekian* [1993], who showed that for long-residence-time reservoirs, the first derivative term dominates in equation (4). The pyrite burial calculation indicates a Paleocene minimum in pyrite burial, followed by an early Eocene peak (Figure 5b). Following the major early Paleogene perturbation, pyrite burial remains relatively constant through the rest of the Cenozoic. Our modeling shows that even assuming a low early Cenozoic sulfate concentration (variable sulfate case), the calculated pyrite burial curve retains its first order features: a significant

decrease in pyrite burial in the Paleocene followed by a prominent maximum in the early Eocene and relative stability throughout the rest of the Cenozoic (Figure 5b).

2.3. Sensitivity Analyses

[16] Models used to calculate the evolution of organic carbon burial from isotopic mass balance are subject to many uncertainties including assumptions about paleoweathering fluxes and changing isotopic fractionation [e.g., *Raymo*, 1997]. Models of pyrite burial are subject to many of the same uncertainties, with added complications particularly when looking at relatively short-term changes, where steady state cannot be assumed. Given these uncertainties, the pyrite burial curves shown in Figure 5b are not unique solutions.

[17] Cenozoic variations in Δ_S , analogous to documented changes in Δ_C [Popp et al., 1989; Hayes et al., 1999], would affect our interpretations of the sulfur isotope record. *Habicht et al.* [2002] showed that Δ_S can be sensitive to $[\text{SO}_4^{2-}]$ but only at extremely low concentrations (< 1 mM), which are probably not relevant to the Cenozoic. *Strauss* [1999] compiled available data for the Phanerozoic evolution of Δ_S based on the difference between $\delta^{34}\text{S}$ of gypsum sulfate and the average $\delta^{34}\text{S}$ of pyrite sulfur at 10 to 100 m.y. resolution. *Strauss* inferred that Δ_S has varied between -14 and -54% since the Precambrian. Holding all other parameters constant, we calculate the variability in Δ_S required to attribute all Cenozoic changes in $\delta^{34}\text{S}$ to Δ_S alone [cf. *Kump*, 1989]. Figure 6 shows that the rapid Eocene rise in $\delta^{34}\text{S}$ would require extreme values of Δ_S (-70 to -170%), values well outside of the observed range in Phanerozoic Δ_S [Strauss, 1999]. Although improved knowledge of Cenozoic-scale variations in Δ_S would improve interpretations of the sulfur isotopic record, it is unlikely that Δ_S has exerted a dominant control on the Cenozoic sulfur curve.

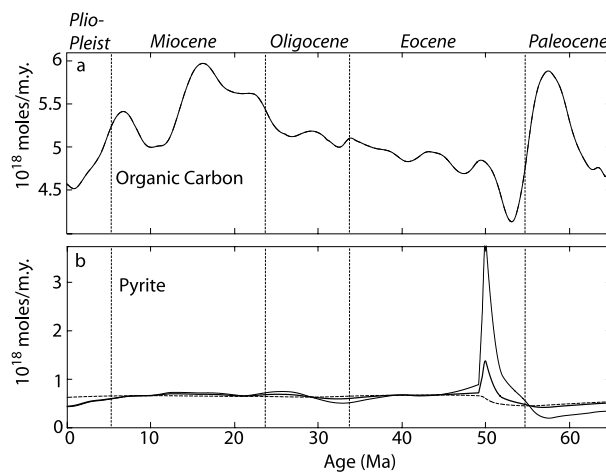


Figure 5. Modeled Cenozoic histories of organic (a) carbon and (b) pyrite burial. In Figure 5b the light line is the constant sulfate case. The bold line shows the calculation based on the variable sulfate case. Dashed curve illustrates the result of a model that assumes isotopic steady state (i.e., differential term in equation (4) set to zero).

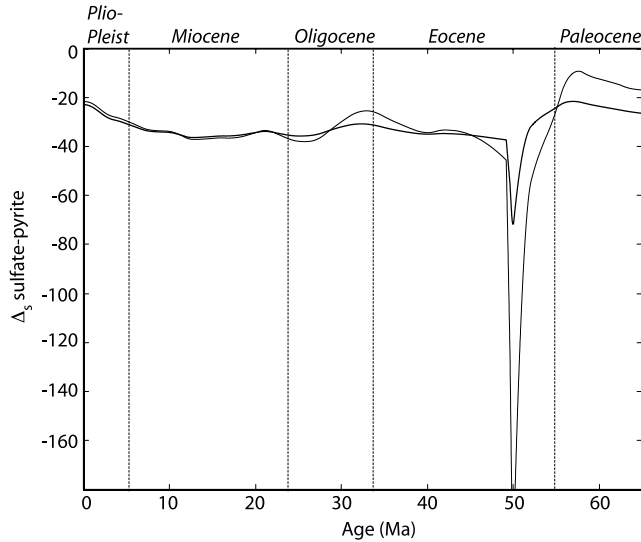


Figure 6. Calculated changes in Δ_S required to explain the Cenozoic sulfur isotope record, assuming all other parameters constant with values summarized in Table 1. The extreme Δ_S values calculated between 55 and 50 Ma are outside of the range in Δ_S inferred for the entire Phanerozoic [Strauss, 1999]. Light line is the constant sulfate case; bold line is the variable sulfate case.

[18] The isotopic value of the input sulfur flux (δ_W^S) is determined by the relative weathering fluxes of sedimentary sulfides (pyrite) and sulfates (gypsum) on land, which are largely unknown [Bluth and Kump, 1994] and thus assumed to be invariant. Additionally, isotopic mass balance cannot distinguish between changes in burial terms (F_{py}) and changes in weathering terms (F_W^S). Holding all other parameters constant, a decrease in the riverine sulfur flux (F_W^S) would drive the marine sulfur isotope mass balance (δ_O^S) toward a more positive value without any change in the pyrite burial flux. Rearranging equation (2) to solve for F_W^S , we can test whether the sulfur isotope record can be explained by changes in the weathering sulfur flux under constant F_{py} . Figure 7 shows that regardless of M_O^S evolution, the riverine flux would have to decrease dramatically near the Paleocene-Eocene boundary, and ultimately attain negative values of F_W^S , which is mathematically equivalent to net pyrite burial. This result shows that a change in the riverine flux cannot alone account for the sulfur isotope record.

[19] Furthermore, a change in global weathering fluxes would affect both the S and C cycles. For example, an increased weathering flux would simultaneously shift both S and C isotope records toward the values of the weathering flux ($\delta_W^C = -4\%$ and $\delta_W^S = +7\%$), with the sulfur response lagging the carbon response for the reasons given above. Such a forcing is inconsistent with the trends that we observe for the Paleogene. In any case, a major change in the riverine sulfur flux (presumably related to a decrease in the global weathering flux) should be evident from weathering proxy records. The marine Sr isotope record is an imperfect weathering proxy, but is nonetheless remarkably

flat throughout this interval [Richter *et al.*, 1992], suggesting no major long-term changes in weathering fluxes in the Paleocene-early Eocene. Peucker-Ehrenbrink *et al.* [1995] suggest that the combination of unchanging $^{87}\text{Sr}/^{86}\text{Sr}$ with increasing $^{187}\text{Os}/^{186}\text{Os}$ from 65 to 40 Ma could reflect a gradual increase in the weathering flux of black shales without increased silicate weathering during the early Cenozoic. An increase in weathering fluxes at the PETM has been inferred from Os isotope records, but this was a short-lived event ($\sim 10^4 - 10^5$ years [Ravizza *et al.*, 2001]). Regardless, a weathering-driven explanation of the early Cenozoic S curve would require a dramatic decrease in the terrestrial weathering flux near the Paleocene-Eocene boundary (Figure 7) which is inconsistent with existing radiogenic isotope proxy records. Our intention is not to argue for constant weathering fluxes over the entire Cenozoic, which would be unrealistic. However, our modeling indicates that the simplest explanation for the rapid changes in Paleogene $\delta^{34}\text{S}$ is significant fluctuations in the global rate of pyrite sulfur burial. We believe changes in weathering fluxes had only a secondary effect on the C and S isotope curves. The constant weathering assumption is a simplification.

3. Discussion

3.1. C_{org} and S_{py} Burial Environments

[20] In the modern ocean, carbon and sulfur burial rates are coupled through burial of C_{org} and S_{py} in marine

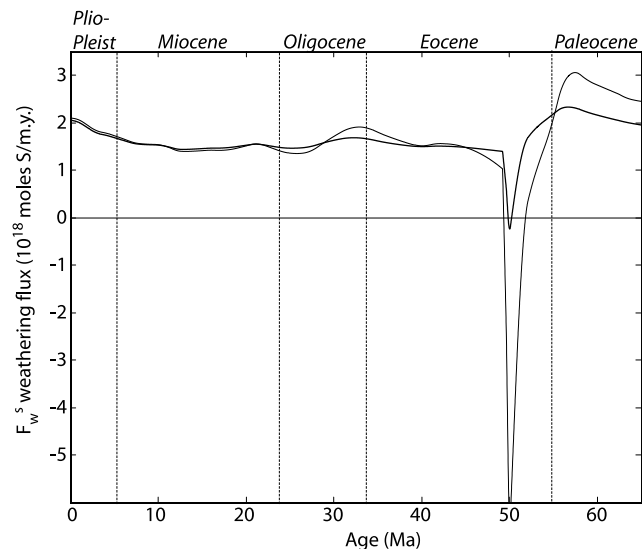


Figure 7. Calculated changes in the riverine sulfur flux required to explain the Cenozoic sulfur isotope record, assuming all other parameters constant with values summarized in Table 1. The fact that both curves contain negative values indicates that a change in weathering flux alone cannot explain the variations in the sulfur isotope curve. Furthermore, a pronounced drop in weathering flux between 55 and 50 Ma is inconsistent with the radiogenic isotope records of this interval [Richter *et al.*, 1992; Peucker-Ehrenbrink *et al.*, 1995]. Light line is the constant sulfate case; bold line is the variable sulfate case.

environments. Pyrite forms in sediments by the reduction of seawater sulfate at the expense of sedimentary organic carbon, and is a strictly anaerobic process. Sedimentary pyrite formation is limited to shelf, deltaic, estuarine, and hemipelagic muds [Berner, 1982]. Hedges and Keil [1995] estimated that 45% of organic matter burial of the oceans takes place in continental shelf environments with an additional 45% in deltaic sediments. Berner [1982] noted that sediments accumulating in shelf and deltaic environments tend to have a remarkably constant C_{org}/S_{py} ratio (~ 7.5 molar, 2.8 weight). Raiswell and Berner [1986] showed through analysis of shales that this ratio has been maintained throughout the Phanerozoic. Berner and Raiswell [1983] attributed this ratio to fixed proportions of reactive (sulfide producing) versus refractory carbon in marine sediments. Alternatively, the constant C/S ratio in normal marine sediments may be related to fixed proportions of iron oxyhydroxides and organic carbon sorbed to fine grained minerals [Berner, 1984; Hedges and Keil, 1995]. Regardless of mechanism, the global rate of pyrite burial is largely determined by the rate of shelf-deltaic organic carbon burial.

[21] The relationship between organic carbon and pyrite burial can change when the locus of carbon burial shifts away from normal shelf-deltaic environments [Berner and Raiswell, 1983]. Several environments inhibit the burial of pyrite. Among these are deep ocean sediments, where sulfate reduction may be limited due to the presence of oxygen or lack of reactive organic matter, shallow water calcareous sediments, where pyrite formation may be limited by the availability of dissolved iron, and terrestrial environments (soils, swamps, and coal basins), where sulfate is in limited supply [Berner, 1982]. In contrast, pyrite burial rates are high in euxinic environments, where pyrite may form in the water column [Raiswell and Berner, 1985]. Raiswell and Berner [1985] calculated a maximum in global C_{org}/S_{py} burial ratio (up to 50 molar ratio) in the Permian/Carboniferous based on modeling C and S isotopic records. The peak at the Permian/Carboniferous boundary coincides with a peak in recoverable coal resources of the same age, supporting the hypothesis that a change in the dominant locus of organic carbon burial to terrigenous environments should be reflected in marine carbon and sulfur isotope records.

[22] Changes in eustatic sea level should exert an important control over organic carbon burial environments. For example, Schlunz *et al.* [1999] showed that organic carbon burial in the Amazon fan system is controlled by glacioeustatic sea level changes. During glacial sea level low stands, terrestrial organic carbon bypasses the continental shelf and is channeled through the Amazon Canyon and buried in the deep sea fan. During interglacial high stands, organic carbon burial is dominated by autochthonous marine organic carbon in the shelf environment. Weissert *et al.* [1998] noted a correlation between marine transgressions and three positive carbon isotope excursions in the Cretaceous. In their model, these positive C excursions are related to both an increase in organic carbon burial (as black shales) and a decrease in carbonate burial, related to drowning of carbonate platforms by rising sea level.

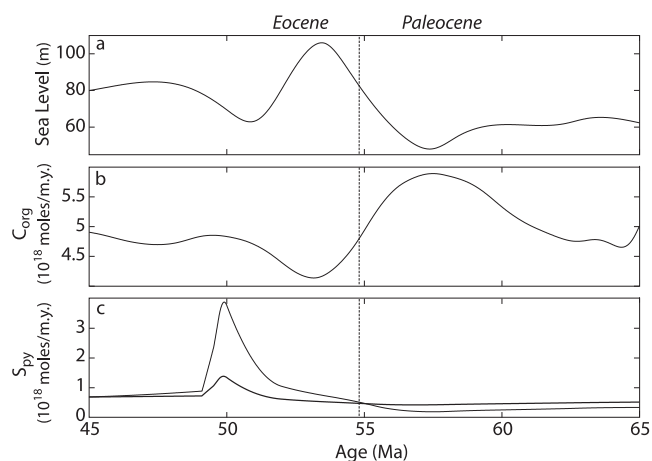


Figure 8. Relationship between early Cenozoic eustatic sea level [Miller *et al.*, 1997] (units in meters above present level, curve smoothed with a cubic smoothing spline) and calculated organic carbon burial and pyrite burial (light line is constant sulfate case; bold line is variable sulfate case). The maximum in organic carbon burial coincided with a minimum in sea level. C_{org} burial dropped off as sea level rose. Pyrite burial was low during the C_{org} burial maximum, began to rise slightly as sea level rose, and then rose sharply following the early Eocene sea level maximum.

[23] High-resolution eustatic sea level records for the Paleogene are now becoming available as a result of the New Jersey Coastal Plain Drilling Project [Miller *et al.*, 1997, 1998]. These records show a long term lowering of 100–150 m over the whole Cenozoic, generally attributed to decreasing global mid-ocean ridge volume (but see Rowley [2002]). The New Jersey Margin record, although preliminary [Miller *et al.*, 1997], suggests that significant fluctuations in sea level may have occurred in the late Paleocene to early Eocene (Figure 8), coincident with the important variations in carbon and sulfur isotope records. Sea level dropped slightly from ~ 60 m above present sea level to ~ 40 m throughout the Paleocene, then abruptly rose to $+110$ m during the late Paleocene and early Eocene. Subsequently, sea level dropped back to $+60$ m during the early Eocene. Interestingly, the relationship between sea level and carbon isotopes is opposite that previously seen for Cretaceous excursions. The Paleocene carbon isotope maximum (and inferred peak in C_{org} burial) corresponds to a sea level low stand, and the waning of the isotope maximum (and inferred pulse of pyrite burial) corresponds to an abrupt rise in sea level of ~ 70 m.

[24] We calculate the Cenozoic evolution of the global C_{org}/S_{py} burial ratio (Figure 9) based on the S_{py} and C_{org} burial histories in Figure 5. The calculated C_{org}/S_{py} burial ratio was at a maximum (~ 15 – 30) in the Paleocene, resulting from both low pyrite sulfur burial and high organic carbon burial at this time. During the early Eocene, the situation reversed, and global C_{org}/S_{py} burial ratios attained a minimum (<4) driven by both low C_{org} and very high S_{py} burial fluxes. Simultaneous changes in C_{org} burial, S_{py} burial, C_{org}/S_{py} ratio, and sea level may point to changes

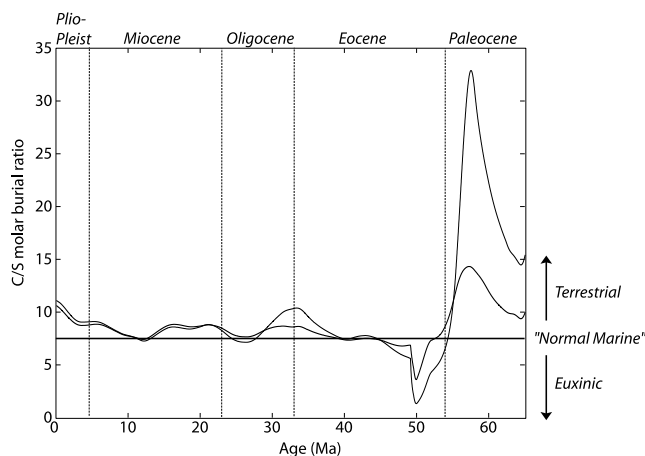


Figure 9. Calculated Cenozoic history of the global organic carbon to pyrite burial ratio, based on pyrite sulfur and organic carbon burial histories shown in Figure 5 (light line is constant sulfate case; bold line is variable sulfate case). Horizontal line shows the organic carbon/pyrite burial ratio typical of normal marine sediments. C/S ratios higher than normal may indicate a shift toward terrestrial organic carbon burial environments, while below-normal C/S ratios may indicate a shift toward euxinic marine carbon burial environments.

in dominant organic carbon burial environments during the Paleocene and Eocene. High $C_{\text{org}}/S_{\text{py}}$ burial ratios may represent terrestrial or open ocean burial environments, while low $C_{\text{org}}/S_{\text{py}}$ ratios most likely represent burial in euxinic environments.

3.2. Role of Marine Organic Carbon Burial

[25] Our model suggests that global organic carbon burial increased ~ 20 – 30% during the Paleocene Carbon Isotope Maximum while pyrite burial decreased at the same time. Below we will argue that a terrestrial mechanism best explains this scenario. Because previous workers have explained the Paleocene carbon isotope maximum via changes in the marine carbon cycle [Corfield and Cartlidge, 1992; Thompson and Schmitz, 1997], we discuss our reasoning for discounting several marine-based scenarios.

[26] Positive carbon isotope excursions in the Cretaceous record tend to correlate with widespread deposition of black shales [Arthur *et al.*, 1985]. In contrast, lack of evidence for abundant organic-carbon rich marine sediments was an early indication that the Paleocene carbon isotope maximum might reflect a pulse of terrestrial, rather than marine organic carbon burial [Oberhansli and Hsu, 1986; Oberhansli and Perch-Nielsen, 1990]. Meyers and Dickens [1992] noted that the Paleocene was a time of low organic carbon accumulation throughout the Indian Ocean basin. Interestingly, the only notable exceptions are the occurrence of sediments with $\sim 0.5\%$ organic carbon on Broken Ridge, which was inferred to be of terrigenous origin, and deposits of Paleocene brown coal on a now submerged portion of Ninetyeast Ridge

[Meyers and Dickens, 1992]. Some examples of Paleocene organic carbon rich marine sediments do exist, among these sediments of the western North Pacific recovered by DSDP Leg 43. Black clays, which are abundant in mid-Cretaceous sediments of the western North Atlantic, reappear at some sites in mid-Paleocene sediments [Tucholke and Vogt, 1979]. These abyssal sediments contain up to 1.3% organic carbon and are interpreted to reflect poorly ventilated deep waters [Tucholke and Vogt, 1979]. The late Paleocene Waipawa Formation in New Zealand [Killops *et al.*, 2000] is another example. These organic carbon rich rocks (locally up to 9 wt% organic carbon) are inferred to have formed in a dysaerobic shelf environment that developed in response to regional upwelling [Killops *et al.*, 2000]. The Waipawa Formation contains abundant sulfur [Killops *et al.*, 2000] and therefore does not represent the high organic carbon, low sulfide burial environment inferred from our model to dominate the Paleocene. Perhaps the most notable example of Paleocene black shales occurs in the southern Tethyan margin. These rocks contain up to 2.7% organic carbon but are entirely restricted to the PETM event [Speijer and Wagner, 2002]. These black shales are therefore not pertinent to the discussion of the broader Paleocene carbon cycle, but are nonetheless interesting as they may reflect a response of the ocean-atmosphere system to massive input of carbon at the PETM [Speijer and Wagner, 2002].

[27] Corfield and Cartlidge [1992] cited an increase in planktonic-benthic foraminiferal $\delta^{13}\text{C}$ gradients as evidence for increased marine productivity during the Paleocene. Their arguments were made on the basis of changes in the $\delta^{13}\text{C}$ gradient between *Morozovella* (planktic) and *Subbotina* (deeper water planktic) or *Nuttallides* (benthic). More recent work by D'Hondt *et al.* [1994] has shown that Paleocene planktic foram species *Morozovella* and *Acarinina* were likely photosymbiotic, and argued that tests of these foraminifers may have been consistently ^{13}C enriched relative to contemporaneous seawater. They cautioned strongly against paleoproductivity interpretations based on these species. Interestingly, the late Paleocene radiation of photosymbiont-bearing planktonic foraminifera (i.e., *Morozovella* and *Acarinina* [Norris, 1991]) might be viewed as supporting a transition to globally lower marine productivity rather than higher. Photosymbiosis as a survival strategy is generally viewed as advantageous in oligotrophic environments where nutrient availability is limited [Norris, 1996].

[28] Taking pyrite burial as a proxy for burial of marine organic carbon in shelf-delta environments [Kump, 1993] we interpret the sulfur isotope record as evidence for a $\sim 50\%$ decrease in shelf carbon burial during the Paleocene. However, a net shift of organic carbon sedimentation to pyrite-lean pelagic settings might explain the combination of increased organic carbon burial and very high $C_{\text{org}}/S_{\text{py}}$ burial ratios. Such a scenario would require a roughly 4-fold increase in global open-ocean carbon burial to offset a 50% decrease in shelf carbon burial while maintaining a 20–30% net increase in C_{org} burial. This scenario is in a sense consistent with the dramatic early Paleocene to late Paleocene increase (6-fold) in organic carbon burial in oligotrophic regions of the ocean proposed by Thompson and

Schmitz [1997]. However, *Thompson and Schmitz* [1997] argued for an overall global doubling in marine organic carbon burial, which is much greater than our estimate. Their conclusions are based on an observed increase in the paleoproductivity proxy “excess Ba” at several DSDP sites, which provides indirect, qualitative evidence for changes in organic carbon burial. A more troubling complication with this interpretation is that they are essentially arguing for a doubling in the global Ba sink that was maintained for at least 4 m.y. Given that the marine residence time for Ba is only 8 k.y., it is not clear what a sustained increase Ba_{excess} might mean in terms of productivity [e.g., *Dickens et al.*, 2003]. Increased Ba_{excess} would require an increase in the Ba input (weathering) flux, unless the observed increase in Ba_{excess} was balanced by Ba_{excess} decreases elsewhere in the Paleocene ocean that have yet to be measured. Finally, this explanation (a quadrupling of the open-ocean organic carbon burial rate) is viable only if it doesn't provide sufficient organic matter to support significant pyrite production, in which case the C/S ratio would be diminished.

[29] Finally, tropical river-dominated ocean margins (e.g., Amazon [*Aller et al.*, 1986, 1996; *Aller and Blair*, 1996] and Gulf of Papua [*Aller et al.*, 2003]) are an additional carbon burial environment that tend to have $C_{\text{org}}/S_{\text{py}}$ burial ratios higher than the canonical marine shelf sediment value [*Berner*, 1982]. Sedimentary C/S ratios of ~ 20 (molar) are typical of the Amazon shelf [*Aller and Blair*, 1996]. Ratios of 10–20 are also seen in the Gulf of Papua, another tropical shelf dominated by riverine processes and physical reworking [*Aller et al.*, 2003]. However, in this case, C/S ratios decrease offshore, and at depths of >45 m, are more typical of normal shelf sediments (e.g., 8 mole ratio). *Aller et al.* [2003] suggest that these high $C_{\text{org}}/S_{\text{py}}$ burial environments are most likely to be associated with tropical weathering during periods of high sea level stand. This mechanism is inconsistent with our observation that organic carbon burial waned during the late Paleocene as sea level rose. It is also not clear that increased organic carbon burial in these environments could produce global C/S ratios as high as 15–30 (Figure 9).

3.3. Role of Terrestrial Organic Carbon Burial

[30] Dominance of terrestrial organic carbon burial could explain why the Paleocene Carbon Isotope Maximum does not apparently correlate to widespread black shale deposition, and does coincide to a calculated maximum in global $C_{\text{org}}/S_{\text{py}}$ burial ratio. We can test this hypothesis for consistency with the geologic record of worldwide coal distribution. Although compiling global statistics on coal resources is notoriously difficult, *Duff* [1987] estimates that half of the world's known coal resources are of Mesozoic-Tertiary age. Important Tertiary coal deposits are found in Europe, east-central and southern Australia, southern and southeastern Asia, the Urals, Siberia, and Pakistan [*Ross and Ross*, 1984; *Shah et al.*, 1993; *Baqri* 1997]. *Ross and Ross* [1984] estimate that 60% of economic Tertiary coals are North American, dominantly located in the western plains and Cordillera. Late Paleocene coals are among the thickest in the entire geologic record [*Shearer et al.*, 1995; *Retallack et al.*, 1996]. The late Paleocene Fort Union

Formation, located in the Montana-Wyoming Powder River Basin contains some of the most significant post-Paleozoic coals in North America [*Ellis et al.*, 1999]. The Wyodak-Anderson member alone contains an estimated 550 Gt economically recoverable coal in beds as much as 60 m thick [*Ellis et al.*, 1999]. Documented Paleocene coal fields in Russia [*Crosdale et al.*, 2002] and Pakistan [*Jaleel et al.*, 1999] tend to have somewhat thinner seams (up to 20 m) and smaller reserves (175 Gt, Thar coalfield, Pakistan) than the Wyodak example but are still significant examples of Paleocene lignite deposits.

[31] Our modeling suggests that the Paleocene Carbon Isotope Maximum can be accounted for by net burial of 1.25×10^{18} moles C during the mid to late Paleocene. For scale, we note that the modern terrestrial biosphere contains 0.17×10^{18} moles C in both living biomass and soil carbon [*Schlesinger*, 1997]. *Beerling* [2000] modeled the evolution of the terrestrial carbon cycle and suggested that the late Paleocene terrestrial biomass and soils contained 0.24×10^{18} moles C, which is 30% larger than today's inventory. The thick Paleocene coal deposits suggest that a significant fraction of this terrestrial carbon stock was buried, rather than remineralized on short time scales. Using the Paleocene Fort Union coal average of 36% carbon [*Ellis et al.*, 1999], 46,000 Gt of coal burial would be required to account for 1.25×10^{18} moles of net C burial. Since $>1\%$ of this amount (i.e., 550 Gt) is presently available as recoverable deposits in one member alone of the Paleocene Fort Union Formation, it seems reasonable that coal deposition could account for the Paleocene Carbon Isotope Maximum. Furthermore, Fort Union Paleocene coals are extremely sulfide-poor. *Ellis et al.* [1999] estimate that the Wyodak-Anderson member averages 0.1% pyrite. This amounts to a molar $C_{\text{org}}/S_{\text{py}}$ ratio of ~ 1800 . Even if this extreme ratio is not typical of Paleocene coals (e.g., Paleocene Hangu Formation coals of Pakistan have molar C/S ratios of ~ 34 [*Shah et al.*, 1993]), it clearly would contribute to globally averaged elevated $C_{\text{org}}/S_{\text{py}}$ ratios during the Paleocene.

3.4. A Paleocene-Eocene “Global Conflagration”?

[32] The Paleocene-Eocene boundary is marked by a pronounced, well-documented short-term excursion in both carbon and oxygen isotopic records. One explanation for the negative carbon excursion accompanying the Paleocene-Eocene Thermal Maximum is rapid release of methane from gas hydrates on continental slopes [e.g., *Dickens et al.*, 1995]. While an active methane subcycle is certainly an important part of the global carbon cycle [*Dickens*, 2001], and to a lesser extent, the global sulfur cycle [*D'Hondt et al.*, 2002], here we propose an alternative explanation for the events surrounding the PETM that does not call upon methane at all.

[33] If the Paleocene was as we have suggested a time of widespread terrestrial organic carbon burial, it is worth considering whether the abrupt negative carbon isotope excursion at the PETM might have a terrestrial, rather than marine, origin. One possibility is the rapid oxidation of terrestrial organic carbon as late Paleocene coal-forming basins waned. Rampant wildfires, in a form of “global

conflagration,” as an oxidative weathering mechanism could rapidly return a large amount of isotopically light carbon to the Paleocene-Eocene atmosphere. The role of wildfire in the global carbon cycle has been underappreciated. For example, droughts resulting from the 1997 El Niño event caused dramatic burning of Indonesian peatlands. The magnitude of carbon release from these fires was estimated between 0.7 and 2.1×10^{14} moles C, comparable to annual global carbon uptake by the terrestrial biosphere [Page et al., 2002]. Page et al. [2002] suggested that burning of the top ~ 0.5 m of peat covering a small part of Earth’s surface (20 Mha) may have been largely responsible for the largest annual increase in atmospheric CO_2 in almost 50 years of instrumental records.

[34] Dickens [2001] argued that accounting for the -2.5% PETM carbon excursion by isotopically normal (e.g., -22%) organic carbon would require the release of 0.7×10^{18} moles C in 10,000 years, approximately half of our calculated Paleocene growth of the sedimentary organic carbon reservoir. This amounts to an average carbon release by burning of 0.7×10^{14} moles C/y, which is within the range estimated for Indonesia in 1997, and perhaps not unreasonable given the widespread occurrence of unusually thick peatlands inferred from the Paleocene coal record. Interestingly, Crosdale et al. [2002] noted that some Paleocene Russian coals are unusually rich in inertinite, and inferred that fire played an important role in Paleocene peatlands of the Zeya-Bureya Basin. Unusually high concentrations of macroscopic charcoal have been identified in lignite beds at the Paleocene-Eocene boundary in southern England [Scott, 2000; Collinson, 2001; Collinson et al., 2003] suggesting that wildfire could have contributed to the observed abrupt negative carbon isotope excursion.

[35] What might cause such sustained wildfires? One possibility is that Paleocene net growth of the sedimentary organic carbon reservoir would have increased atmospheric O_2 , thus increasing the susceptibility of peatlands to burning [Watson et al., 1978]. Net burial of 1.25×10^{18} moles C would result in an addition of 1.25×10^{18} moles O_2 to Earth’s atmosphere. However, because the atmospheric O_2 reservoir is large (38×10^{18} moles at present), it isn’t clear that this increase would be significant enough to increase the susceptibility of peatlands to fire. Furthermore, our model suggests that Paleocene sulfide burial was net negative, i.e., the weathering flux of sedimentary pyrite was larger than the pyrite burial flux. Thus the Paleocene sulfur cycle was likely a net sink of O_2 and the net addition of O_2 to the Paleocene atmosphere was less than 1.25×10^{18} moles.

[36] A more likely explanation may be related to late Paleocene climate change. Page et al. [2002] suggested that it was the unusually long El Niño dry season that caused the 1997 Indonesian fires to spread out of control. A shift toward a drier climate during the late Paleocene could plausibly trigger widespread burning of abundant Paleocene peatlands. Clay mineral assemblages of Tethyan sediments indicate a progressive change from high rainfall in the early Paleocene to a more arid climate in the late Paleocene and early Eocene [Bolle and Adatte, 2001]. The drying trend,

inferred from decreasing kaolinite abundance in six Tethyan sedimentary sections, is briefly interrupted in most sequences by a kaolinite-rich layer at the PETM which may reflect a pulse of increased chemical weathering in response to elevated CO_2 , warmth, and humidity [Gibson et al., 2000; Bolle and Adatte, 2001]. Fossil leaf morphology may also be used as a proxy for Paleocene-Eocene paleoprecipitation [Wolfe, 1993, 1994; Wilf et al., 1998; Wilf, 2000], but interpretations are controversial [Wolfe et al., 1999], and at present there are not enough data to make global generalizations. The evidence from Wyoming is equivocal with respect to our hypothesis: humid conditions apparently prevailed during the late Paleocene, but the long-term trend from the late Paleocene into the early Eocene seems to be warming and drying [Wilf, 2000]. We suggest that abundant, thick peatlands, a trend toward increased aridity, and a major change in atmospheric circulation [Rea et al., 1990] may have triggered a period of increased wildfire that provides an additional mechanism to explain the PETM event.

3.5. Early Eocene Pyrite Burial

[37] Our calculated pyrite burial flux increases rapidly across the Paleocene-Eocene boundary to a peak in the early to middle Eocene. We interpret the early Eocene maximum in pyrite sulfur burial to be a consequence of several factors. High-latitude (or in general, bottom water source area) warming would result in a generally dysoxic ocean (as in the late Permian [e.g., Hotinski et al., 2000]). This interpretation is supported by the analysis of Kaiho [1991] who used the species distribution of benthic foraminifera to calculate an oxygen index, reflecting the dissolved oxygen content of the deep ocean for the whole Cenozoic. Kaiho’s [1991] oxygen index drops dramatically from relatively high values (oxygenated) during the Paleocene to a Cenozoic low at the Paleocene-Eocene boundary, and remains low until the middle Eocene.

[38] Early Eocene sea level rise increased the global area of flooded continental shelves, where pyrite burial is most important. Early Eocene C_{org} burial rates were low, while S_{py} burial rates were high, suggesting the predominance of carbon burial in euxinic environments at this time. Geologic evidence for such environments exists in rocks such as the London Clay, which is an extremely pyrite-rich transgressive shale that was deposited in the early Eocene North Sea Basin [King, 1981; Newell, 2001].

4. Conclusions

[39] Modeling the coevolution of the exogenic carbon and sulfur cycles can significantly improve our understanding of the evolution of the global carbon cycle. We interpret stable C and S isotope records as evidence for high Paleocene organic carbon burial rates accompanied by remarkably low pyrite sulfur burial rates. Although we cannot absolutely rule out an increase in marine organic carbon burial, we interpret this as evidence that Paleocene organic carbon burial was dominated by terrestrial environments, where sulfate was in limited supply. Coals of Paleocene age appear to be sufficiently voluminous to account for the net burial of

1.25×10^{18} moles C inferred from isotopic mass balance models. Furthermore, these coals have low sulfur content, consistent with high $C_{\text{org}}/S_{\text{py}}$ burial ratios.

[40] The $\delta^{34}\text{S}$ record contains a rapid shift in the early Eocene that we interpret as a pulse of pyrite burial in globally widespread euxinic environments. The calculated magnitude of this pulse is dependent on the mass of the marine sulfate reservoir during the Paleocene-Eocene, which may have been smaller than at present. The further development of proxy records of seawater $[\text{SO}_4^{2-}]$ will be an important complement to $\delta^{34}\text{S}$ records in reconstructions of the evolution of the exogenic sulfur cycle.

[41] The inference of a Paleocene carbon cycle dominated by terrestrial organic carbon burial raises the possibility that the changes in the terrestrial C reservoir also contributed to

the short-term negative carbon isotope excursion at the Paleocene-Eocene Thermal Maximum. As an alternative or in addition to gas hydrates, we propose that a “global conflagration,” sustained burning of accumulated Paleocene terrestrial organic carbon in response to increased aridity may have contributed to the PETM negative carbon isotope excursion. This hypothesis can be tested by further study of the occurrence of fossil charcoal in Paleocene-Eocene boundary terrestrial sediments.

[42] **Acknowledgments.** ACK, LRK, and MAA acknowledge support from the NASA Astrobiology Institute. LRK also acknowledges the support of the NSF Biocomplexity in the Environment Program. We thank Ellen Thomas for providing a revised age model for the Cenozoic sulfur isotope record. This paper was much improved thanks to thorough reviews by Jerry Dickens and an anonymous referee.

References

- Aller, R. C., and N. E. Blair, Sulfur diagenesis and burial on the Amazon shelf: Major control by physical sedimentation processes, *Geo Mar. Lett.*, 16, 3–10, 1996.
- Aller, R. C., J. E. Mackin, and R. T. Cox Jr., Diagenesis of Fe and S in Amazon inner shelf muds: Apparent dominance of Fe reduction and implications for the genesis of ironstones, *Cont. Shelf Res.*, 6, 263–289, 1986.
- Aller, R. C., N. E. Blair, Q. Xia, and P. D. Rude, Remineralization rates, recycling, and storage of carbon in Amazon shelf sediments, *Cont. Shelf Res.*, 16, 753–786, 1996.
- Aller, R. C., A. Hannides, C. Heilbrun, and C. Panzeca, Coupling of early diagenetic processes and sedimentary dynamics in tropical shelf environments: The Gulf of Papua deltaic complex, *Cont. Shelf Res.*, in press, 2003.
- Arthur, M. A., W. E. Dean, and S. O. Schlanger, Variations in the global carbon cycle during the Cretaceous related to climate, volcanism, and changes in atmospheric CO_2 , in *The Carbon Cycle and Atmospheric CO_2 : Natural Variations Archean to Present*, *Geophys. Monogr. Ser.*, vol. 32, edited by E. T. Sundquist and W. S. Broecker, pp. 504–529, AGU, Washington, D. C., 1985.
- Baqri, S. R. H., The distribution of sulfur in the Palaeocene coals of the Sindh Province of Pakistan, in *European Coal Geology and Technology*, edited by R. A. Gayer and J. Pesek, *Geol. Soc. Spec. Publ.*, 125, 237–243, 1997.
- Beerling, D. J., Increased terrestrial carbon storage across the Palaeocene-Eocene boundary, *Palaeogeogr. Palaeoclimatol. Palaeoecol.*, 161, 395–405, 2000.
- Berggren, W. A., D. V. Kent, C. C. Swisher III, and M.-P. Aubry, A revised Cenozoic geochronology and chronostratigraphy, in *Geochronology, Time Scales and Global Stratigraphic Correlation*, edited by W. A. Berggren et al., *Spec. Publ. SEPM Sediment. Geol.*, 54, 129–212, 1995.
- Berner, R. A., Burial of organic carbon and pyrite sulfur in the modern ocean: Its geochemical and environmental significance, *Am. J. Sci.*, 282, 451–473, 1982.
- Berner, R. A., Sedimentary pyrite formation: An update, *Geochim. Cosmochim. Acta*, 48, 605–615, 1984.
- Berner, R. A., and R. Raiswell, Burial of organic carbon and pyrite sulfur in sediments over Phanerozoic time: A new theory, *Geochim. Cosmochim. Acta.*, 47, 855–862, 1983.
- Bluth, G. J. S., and L. R. Kump, Lithologic and climatologic controls of river chemistry, *Geochim. Cosmochim. Acta*, 58, 2341–2359, 1994.
- Bolle, M. P., and T. Adatte, Palaeocene early Eocene climatic evolution in the Tethyan realm: Clay mineral evidence, *Clay Miner.*, 36, 249–261, 2001.
- Bralower, T. J., J. C. Zachos, E. Thomas, M. Parrow, C. K. Paull, D. C. Kelly, I. Premoli Silva, W. V. Sliter, and K. C. Lohmann, Late Paleocene to Eocene paleoceanography of the Equatorial Pacific Ocean: Stable isotopes recorded at Ocean Drilling Program Site 865, Allison Guyot, *Paleoceanography*, 10, 841–865, 1995.
- Cande, S. C., and D. V. Kent, Revised calibration of the geomagnetic polarity timescale for the Late Cretaceous and Cenozoic, *J. Geophys. Res.*, 100(B4), 6093–6095, 1995.
- Carpenter, S. J., and K. C. Lohmann, Carbon isotope ratios of Phanerozoic marine cements: Re-evaluating the global carbon and sulfur systems, *Geochim. Cosmochim. Acta.*, 61, 4831–4846, 1997.
- Collinson, M. E., Early Paleogene floras and land environments, paper presented at Climate and Biota of the Early Paleogene, International Meeting, Nat. Sci. Found., Powell, Wyo., July 2001.
- Collinson, M. E., J. J. Hooker, and D. R. Grocke, Cobham lignite bed and penecontemporaneous macrofloras of southern England: A record of vegetation and fire across the Paleocene-Eocene Thermal Maximum, in *Causes and Consequences of Globally Warm Climates in the Early Paleogene*, edited by S. L. Wing et al., *Spec. Pap. Geol. Soc. Am.*, 369, 333–349, 2003.
- Corfield, R. M., Palaeocene oceans and climate: An isotopic perspective, *Earth Sci. Rev.*, 37, 225–252, 1994.
- Corfield, R. M., The oxygen and carbon isotopic context of the Paleocene/Eocene epoch boundary, in *Late Paleocene-Early Eocene Climatic and Biotic Events in the Marine and Terrestrial Records*, edited by M.-P. Aubry, S. G. Lucas, and W. A. Berggren, pp. 124–137, Inst. des Sci. de l’Evol., Univ. de Montpellier II, Montpellier, France, 1998.
- Corfield, R. M., and J. E. Cartledge, Oceanographic and climatic implications of the Palaeocene carbon isotope maximum, *Terra Nova*, 4, 443–455, 1992.
- Crosdale, P. J., A. P. Sorokin, K. J. Woolfe, and D. I. M. Macdonald, Inertinite-rich Tertiary coals from the Zeya-Bureya Basin, far eastern Russia, *Int. J. Coal Geology*, 51, 215–235, 2002.
- D’Hondt, S., J. Zachos, and G. Schultz, Stable isotopic signals and photosymbiosis in late Paleocene planktic foraminifera, *Paleobiology*, 20, 391–406, 1994.
- D’Hondt, S., S. Rutherford, and A. J. Spivack, Metabolic activity of subsurface life in deep-sea sediments, *Science*, 295, 2067–2070, 2002.
- deBoor, C., *Spline Toolbox for Use With MATLAB*, The Math Works, Natick, Mass., 1999.
- Dickens, G., Modeling the global carbon cycle with a gas hydrate capacitor: Significance for the Late Paleocene Thermal Maximum, in *Natural Gas Hydrates: Occurrence, Distribution, and Detection*, *Geophys. Monogr. Ser.*, vol. 124, edited by C. K. Paull and W. P. Dillon, pp. 19–38, AGU, Washington, D. C., 2001.
- Dickens, G. R., J. R. O’Neil, D. K. Rea, and R. M. Owen, Dissociation of oceanic methane hydrate as a cause of the carbon isotope excursion at the end of the Paleocene, *Paleoceanography*, 10, 965–971, 1995.
- Dickens, G., T. Fewless, E. Thomas, and T. J. Bralower, Excess barite accumulation during the Paleocene-Eocene Thermal Maximum: Massive input of dissolved barium from sea-floor gas hydrate reservoirs, in *Causes and Consequences of Globally Warm Climates in the Early Paleogene*, edited by S. L. Wing et al., *Spec. Pap. Geol. Soc. Am.*, 369, 11–23, 2003.
- Duff, P. M. D., Mesozoic and Tertiary coals: A major world energy resource, *Mod. Geology*, 11, 29–50, 1987.
- Ellis, M. S., G. L. Gunther, A. M. Ochs, S. B. Roberts, E. M. Wilde, J. H. Schuenemeyer, H. C. Power, G. D. Stricker, and D. Blake, Coal resources, Powder River basin, *U.S. Geol. Surv. Prof. Pap.*, P 1625-A, 32 pp., 1999.
- Garrels, R. M., and A. Lerman, Coupling of sedimentary sulfur and carbon cycles—An improved model, *Am. J. Sci.*, 284, 989–1007, 1984.

- Gibson, T. G., L. M. Bybell, and D. B. Mason, Stratigraphic and climatic implications of clay mineral changes around the Paleocene/Eocene boundary of the northeastern US margin, *Sediment. Geol.*, 134, 65–92, 2000.
- Habicht, K. S., M. Gade, B. Thamdrup, P. Berg, and D. E. Canfield, Calibration of sulfate levels in the Archean ocean, *Science*, 298, 2372–2374, 2002.
- Hayes, J. M., H. Strauss, and A. J. Kaufman, The abundance of ^{13}C in marine organic matter and isotopic fractionation in the global biogeochemical cycle of carbon during the past 800 Ma, *Chem. Geol.*, 161, 103–125, 1999.
- Hedges, J. I., and R. G. Keil, Sedimentary organic-matter preservation—An assessment and speculative synthesis, *Mar. Chem.*, 49, 81–115, 1995.
- Holser, W. T., M. Schidlowski, F. T. Mackenzie, and J. B. Maynard, Biogeochemical cycles of carbon and sulfur, in *Chemical Cycles in the Evolution of the Earth*, edited by C. B. Gregor et al., pp. 105–173, John Wiley, New York, 1988.
- Horita, J., H. Zimmermann, and H. D. Holland, Chemical evolution of seawater during the Phanerozoic: Implications from the record of marine evaporites, *Geochim. Cosmochim. Acta*, 66, 3733–3756, 2002.
- Hotinski, R. M., L. R. Kump, and R. G. Najjar, Opening Pandora's box: The impact of open system modeling on interpretations of anoxia, *Paleoceanography*, 15, 267–279, 2000.
- Jaleel, A., G. S. Alam, and S. A. A. Shah, Coal resources of Thar, Sindh, Pakistan, report, vol. 110, 59 pp., Geol. Surv. of Pakistan, 1999.
- Kaiho, K., Global changes of Paleogene aerobic/anaerobic benthic foraminifera and deep-sea circulation, *Palaeoogeogr. Palaeoecol.*, 83, 65–85, 1991.
- Killops, S. D., C. J. Hollis, H. E. G. Morgans, R. B. D. Sutherland, and A. Leckie, Paleoenvironmental significance of late Paleocene dysaerobia at the shelf/slope break around New Zealand, *Palaeoogeogr. Palaeoecol.*, 156, 51–70, 2000.
- King, C., The stratigraphy of the London Clay and associated deposits, *Tertiary Res. Spec. Pap.*, 8, 1–158, 1981.
- Kump, L. R., Alternative modeling approaches to the geochemical cycles of carbon, sulfur, and strontium isotopes, *Am. J. Sci.*, 289, 390–410, 1989.
- Kump, L. R., The coupling of the carbon and sulfur biogeochemical cycles over Phanerozoic time, in *Interactions of C, N, P, and S Biogeochemical Cycles and Global Change*, edited by R. Wollast, F. T. Mackenzie, and L. Chou, *NATO ASI Ser., Ser. I*, vol. 14, pp. 475–490, Springer-Verlag, New York, 1993.
- Kump, L. R., and M. A. Arthur, Global chemical erosion during the Cenozoic: Weatherability balances the budgets, in *Tectonic Uplift and Climate Change*, edited by W. F. Ruddiman, pp. 400–426, Plenum, New York, 1997.
- Kump, L. R., and M. A. Arthur, Interpreting carbon-isotope excursions: Carbonates and organic matter, *Chem. Geol.*, 161, 181–198, 1999.
- Kump, L. R., and R. M. Garrels, Modeling atmospheric O_2 in the global sedimentary redox cycle, *Am. J. Sci.*, 286, 337–360, 1986.
- Lowenstein, T. K., M. N. Timofeeff, S. T. Brennan, L. A. Hardie, and R. V. Demicco, Oscillations in Phanerozoic seawater chemistry: Evidence from fluid inclusions, *Science*, 294, 1086–1088, 2001.
- Meyers, P. A., and G. R. Dickens, Accumulations of organic matter in sediments of the Indian Ocean: A synthesis of results from scientific deep sea drilling, in *Synthesis of Results From Scientific Drilling in the Indian Ocean, Geophys. Monogr. Ser.*, vol. 70, edited by R. A. Duncan et al., pp. 295–309, AGU, Washington, D. C., 1992.
- Miller, K. G., T. R. Janacek, M. E. Katz, and D. J. Keil, Abyssal circulation and benthic foraminiferal changes near the Palaeocene/Eocene boundary, *Paleoceanography*, 2, 741–761, 1987.
- Miller, K. G., J. V. Browning, S. F. Pekar, and P. J. Sugarman, Cenozoic evolution of the New Jersey coastal plain: Changes in sea level, tectonics, and sediment supply, *Proc. Ocean Drill. Program, Sci. Results*, 150X, 361–373, 1997.
- Miller, K. G., G. S. Mountain, J. V. Browning, M. Kominz, P. J. Sugarman, N. Christie-Blick, M. E. Katz, and J. D. Wright, Cenozoic global sea level, sequences, and the New Jersey transect: Results from coastal plain and continental slope drilling, *Rev. Geophys.*, 36, 569–601, 1998.
- Newell, A. J., Construction of a Palaeogene tide-dominated shelf: Influence of Top Chalk topography and sediment supply (Wessex Basin, UK), *J. Geol. Soc. London*, 158, 379–390, 2001.
- Norris, R. D., Biased extinction and evolutionary trends, *Paleobiology*, 17, 388–399, 1991.
- Norris, R. D., Symbiosis as an evolutionary innovation in the radiation of Paleocene planktic foraminifera, *Paleobiology*, 22, 461–480, 1996.
- Oberhansli, H. and K. J. Hsu, Paleocene-Eocene paleoceanography, in *Mesozoic and Cenozoic Oceans*, Geodyn. Ser., vol. 15, pp. 85–100, AGU, Washington, D. C., 1986.
- Oberhansli, H., and K. Perch-Nielsen, The Paleocene ^{13}C -event: Was it due to changes in the storage rate of terrestrial biomass?, *Veroff. Uebersee Mus. Bremen Reihe A*, A10, 99–112, 1990.
- Page, S. E., F. Siegart, J. O. Rieley, H. D. V. Boehm, A. Jaya, and S. Limin, The amount of carbon released from peat and forest fires in Indonesia during 1997, *Nature*, 420, 61–65, 2002.
- Paytan, A., and K. R. Arrigo, The sulfur-isotopic composition of Cenozoic seawater sulfate: Implications for pyrite burial and atmospheric oxygen, *Int. Geol. Rev.*, 42, 491–498, 2000.
- Paytan, A., M. Kastner, D. Campbell, and M. H. Thiemens, Sulfur isotopic composition of Cenozoic seawater sulfate, *Science*, 282, 1459–1462, 1998.
- Petsch, S. T., and R. A. Berner, Coupling the geochemical cycles of C, P, Fe, and S: The effect on atmospheric O_2 and the isotopic records of carbon and sulfur, *Am. J. Sci.*, 298, 246–262, 1998.
- Peucker-Ehrenbrink, B., G. Ravizza, and A. W. Hofmann, The marine $^{187}\text{Os}/^{186}\text{Os}$ record of the past 80 million years, *Earth Planet. Sci. Lett.*, 130, 155–167, 1995.
- Popp, B. N., R. Takigiku, J. M. Hayes, J. W. Louda, and E. W. Baker, The post-Paleozoic chronology and mechanism of ^{13}C depletion in primary marine organic matter, *Am. J. Sci.*, 289, 436–454, 1989.
- Raiswell, R., and R. A. Berner, Pyrite formation in euxinic and semi-euxinic sediments, *Am. J. Sci.*, 285, 710–724, 1985.
- Raiswell, R., and R. A. Berner, Pyrite and organic matter in Phanerozoic normal marine shales, *Geochim. Cosmochim. Acta*, 50, 1967–1976, 1986.
- Ravizza, G., R. N. Norris, J. Blusztajn, and M. P. Aubry, An osmium isotope excursion associated with the late Paleocene Thermal Maximum: Evidence of intensified chemical weathering, *Paleoceanography*, 16, 155–163, 2001.
- Raymo, M. E., Carbon cycle models: How strong are the constraints?, in *Tectonic Uplift and Climate Change*, edited by W. F. Ruddiman, pp. 368–381, Plenum, New York, 1997.
- Rea, D. K., J. C. Zachos, R. M. Owen, and P. D. Gingerich, Global change at the Paleocene-Eocene boundary: Climatic and evolutionary consequences of tectonic events, *Palaeoogeogr. Palaeoecol.*, 79, 117–128, 1990.
- Retallack, G. J., J. J. Veevers, and R. Morante, Global coal gap between Permian-Triassic extinction and Middle Triassic recovery of peat-forming plants, *Geol. Soc. Am. Bull.*, 108, 195–207, 1996.
- Richter, F. M., and K. K. Turekian, Simple models for the geochemical response of the ocean to climatic and tectonic forcing, *Earth Planet. Sci. Lett.*, 119, 121–131, 1993.
- Richter, F. M., D. B. Rowley, and D. J. DePaolo, Sr isotope evolution of seawater: The role of tectonics, *Earth Planet. Sci. Lett.*, 109, 11–23, 1992.
- Ross, C. A., and J. R. P. Ross, *Geology of Coal*, 349 pp., John Wiley, Hoboken, N. J., 1984.
- Rowley, D. B., Rate of plate creation and destruction: 180 Ma to present, *Geol. Soc. Am. Bull.*, 114, 927–933, 2002.
- Schlesinger, W. H., Biogeochemistry: An analysis of global change, 588 pp., Academic, San Diego, Calif., 1997.
- Schlunz, B., R. R. Schneider, P. J. Muller, W. J. Showers, and G. Wefer, Terrestrial organic carbon accumulation on the Amazon deep sea fan during the last glacial sea level low stand, *Chem. Geol.*, 159, 263–281, 1999.
- Scott, A. C., The Pre-Quaternary history of fire, *Palaeoogeogr. Palaeoecol.*, 164, 281–329, 2000.
- Shackleton, N. J., The carbon isotope record of the Cenozoic: History of organic carbon burial and of oxygen in the ocean and atmosphere, in *Marine Petroleum Source Rocks*, edited by J. Brooks and A. J. Fleet, *Geol. Soc. Spec. Publ.*, 26, 423–434, 1987.
- Shackleton, N. J., and M. A. Hall, Carbon isotope data from Leg 74 sediments, *Initial Rep. Deep Sea Drill. Proj.*, 74, 613–619, 1984.
- Shackleton, N. J., M. A. Hall, and A. Boersma, Oxygen and carbon isotope data from leg 74 foraminifers, *Initial Rep. Deep Sea Drill. Proj.*, 74, 599–612, 1984.
- Shah, M. R., I. A. Abbasi, M. Haneef, and A. Khan, Nature, origin and mode of occurrence of Hangu-Kachai area coal, district Kohat, NWFP, Pakistan: A preliminary study, *Geol. Bull.* 26, p. 87–94, Univ. of Peshawar, Peshawar, Pakistan, 1993.
- Shearer, J. C., T. A. Moore, and T. D. Demchuk, Delineation of the distinctive nature of Tertiary coal beds, *Int. J. Coal Geol.*, 28, 71–98, 1995.
- Speijer, R. P., and T. Wagner, Sea-level changes and black shales associated with the late Paleocene Thermal Maximum: Organic-geochemical and micropaleontologic evidence from the southern Tethyan margin (Egypt-Israel), in *Catastrophic Events and Mass Extinctions: Impacts and Beyond*, edited by C. Koeberl and K. G. MacLeod, *Spec. Pap. Geol. Soc. Am.*, 356, 533–549, 2002.

- Strauss, H., Geological evolution from isotope proxy signals—Sulfur, *Chem. Geol.*, 161, 89–101, 1999.
- Thompson, E. I., and B. Schmitz, Barium and late Paleocene $\delta^{13}\text{C}$ maximum: Evidence of increased marine surface productivity, *Paleoceanography*, 12, 239–254, 1997.
- Tucholke, B. E., and P. R. Vogt, Western North Atlantic: Sedimentary evolution and aspects of tectonic history, *Initial Rep. Deep Sea Drill. Proj.*, 43, 791–825, 1979.
- Veizer, J., W. T. Holser, and C. K. Wilgus, Correlation of $^{13}\text{C}/^{12}\text{C}$ and $^{34}\text{S}/^{32}\text{S}$ secular variations, *Geochim. Cosmochim. Acta*, 44, 579–587, 1980.
- Watson, A. J., J. E. Lovelock, and L. Margulis, Methanogenesis, fires and the regulation of atmospheric oxygen, *BioSystems*, 10, 293–298, 1978.
- Weissert, H., A. Lini, K. B. Follmi, and O. Kuhn, Correlation of Early Cretaceous carbon isotope stratigraphy and platform drowning events: A possible link?, *Palaeogeogr. Palaeoclimatol. Palaeoecol.*, 137, 189–203, 1998.
- Wilf, P., Late-Paleocene-early Eocene climate changes in southwestern Wyoming, Paleobotanical analysis, *Geol. Soc. Am. Bull.*, 112, 292–307, 2000.
- Wilf, P., S. L. Wing, D. R. Greenwood, and C. L. Greenwood, Using fossil leaves as paleoprecipitation indicators: An Eocene example, *Geology*, 26, 203–206, 1998.
- Wolfe, J. A., A method of obtaining climatic parameters from leaf assemblages, *U.S. Geol. Surv. Bull.*, B 2040, 71 pp., 1993.
- Wolfe, J. A., Tertiary climatic changes at middle latitudes of western North America, *Palaeogeogr. Palaeoclimatol. Palaeoecol.*, 108, 195–205, 1994.
- Wolfe, J. A., K. Uemura, P. Wilf, S. L. Wing, D. R. Greenwood, and C. L. Greenwood, Using fossil leaves as paleoprecipitation indicators: An Eocene example: Comment and reply, *Geology*, 27, 91–92, 1999.
-
- M. A. Arthur and L. R. Kump, Department of Geosciences and NASA Astrobiology Institute, Pennsylvania State University, University Park, PA 16802, USA.
- A. C. Kurtz, Department of Earth Sciences, Boston University, Boston, MA 02215, USA. (kurtz@bu.edu)
- A. Paytan, Department of Geological and Environmental Sciences, Stanford University, Stanford, CA 94305, USA.
- J. C. Zachos, Earth Sciences Department, University of California, Santa Cruz, Santa Cruz, CA 95064, USA.